AAS 15-748

ANALYTICAL ASSESSMENT OF DRAG-MODULATION TRAJECTORY CONTROL FOR PLANETARY ENTRY

Zachary R. Putnam* **and Robert D. Braun†**

Discrete-event drag-modulation trajectory control is assessed for planetary entry using the analytical Allen-Eggers approximate solution to the equations of motion. A control authority metric for drag-modulation trajectory control systems is derived. Closed-form relationships are developed to assess range divert capability, identify jettison condition constraints for limiting peak acceleration and peak heat rate. Discrete-event drag-modulation systems with single stages and an arbitrary number of stages are assessed.

INTRODUCTION

Exerting a measure of control over a planetary entry trajectory during flight is important for many missions, whether used to limit peak acceleration, perform precision landing, or accomplish another objective. Mission designers typically choose initial conditions for a particular trajectory to ensure favorable flight performance. However, even the most perfectly selected initial conditions do not eliminate the need to steer out error during entry caused by uncertainty in vehicle properties, onboard state estimation, and the planetary environment, as well as delivery error. Typically only two vehicle parameters are available to control the vehicle trajectory during atmospheric flight: lift-to-drag ratio and ballistic coefficient.

Deployable hypersonic decelerators currently being developed by NASA enable new options for trajectory control for planetary entry. One such option is drag-modulation trajectory control. Consider the ballistic coefficient, defined as*:

$$\beta = m/\left(C_D S_{ref}\right) \tag{1}$$

The ballistic coefficient may be thought of as the ratio of inertial to drag forces. Decreasing the ballistic coefficient increases the influence of drag forces relative to inertial forces, increasing the rate of energy depletion during atmospheric flight. Increasing the ballistic coefficient has the opposite effect. Therefore, an entry vehicle that can vary its ballistic coefficient is capable of controlling its energy or range in a manner similar to that of a lift-modulation vehicle. Operationally, changing vehicle mass by a significant amount is difficult and undesirable. For an entry vehicle of constant mass m, drag-modulation trajectory control is accomplished by changing the drag area ($C_D S_{ref}$) to change ballistic coefficient and adjust the magnitude of the drag force.

*Research Engineer, School of Aerospace Engineering, Georgia Institute of Technology, 270 Ferst Dr., Atlanta, GA, 30332.

†Professor, School of Aerospace Engineering, Georgia Institute of Technology, 270 Ferst Dr., Atlanta, GA, 30332

*A section on mathematical notation is provided in the sequel.

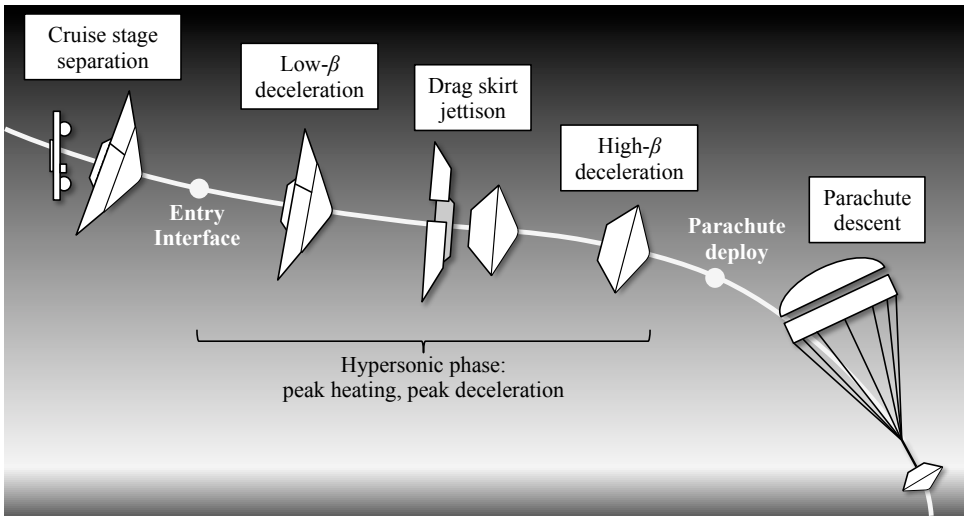

Figure 1. Example drag-modulation system for entry, descent, and landing.

Drag-modulation trajectory control is a prime candidate for use with large, deployable drag areas, such as those envisioned by NASA's Hypersonic Inflatable Aerodynamic Decelerator program. Effector requirements for large, likely flexible, vehicles may make lift modulation infeasible or undesirable. For these types of vehicles, or for missions in which a simpler system is enabling in terms of cost and risk, drag-modulation trajectory control presents a solution that does not require complex effectors or asymmetric flight conditions. The ability to fly at zero angle of attack reduces the criticality of uncertainty in vehicle aerodynamic properties at asymmetric flight conditions; the absence of a reaction control system eliminates concerns about effector latency and jet interaction with a flexible structure and complex wake flow field; the absence of propellant tanks, propellant, and ejectable ballast masses (for c.g. control) greatly simplifies packaging, system integration, and operational complexity. These benefits come at the expense of drag-modulation systems' inability to provide out-of-plane control authority.

Drag-modulation trajectory control is enabled by two technologies: precise approach navigation and deployable hypersonic decelerators. Current deep-space navigation precision results in minimal delivery and knowledge errors at the top of the atmosphere, making out-of-plane control optional in the absence of plane-change or crossrange requirements. Deployable hypersonic decelerators provide a mass-efficient solution to lower the ballistic coefficient and achieve the required ballistic coefficient ratio and control authority.

Discrete-Event Drag-Modulation Trajectory Control

This study examines discrete-event, drag-modulation trajectory control of range during planetary entry, achieved through a series of drag-area jettisons. The jettison events instantly raise ballistic coefficient by reducing the drag area, and may be thought of as adjusting the ratio of inertial to aerodynamic forces such that the desired range is flown. An example of a single-stage drag-modulation entry, descent, and landing system is shown in Fig. 1.

A limited number of studies on drag modulation are available in the literature. Drag modulation has been applied to limiting the rate of increase of acceleration during entry,[1] to orbit phasing and entry targeting,[2] and to track reference trajectories for ballistic missiles.[3] These studies all assumed

drag could be controlled continuously within a given interval. Discrete-event drag modulation has been studied for planetary aerocapture missions at the conceptual level[4–6] and realtime guided performance has been assessed.[7–10] More recently, the feasibility of a single-stage drag modulation system was assessed for precision landing at Mars using a realtime numerical predictor-corrector guidance algorithm.[11] This investigation seeks to identify trends in drag-modulation trajectories through piecewise application of the Allen-Eggers approximate solution for ballistic entry.

Analytical Solutions with Variable Drag

Phillips and Cohen investigated both single-stage and continuously-variable drag-modulation systems as a means to reduce peak acceleration during entry.[12] They were able to develop analytical expressions for minimum peak acceleration for both types systems. These results are rederived and extended below. In 1960, Robinson presented an analysis of continuously-variable systems identical to that of Phillips and Cohen.[13] Randall also studied discrete, single-stage drag-modulation systems, but from the standpoint of modeling break-up during reentry.[14] His work was primarily focused on determining the effect of the initial trajectory on the trajectory of an ejected portion of a body. Warden studied entry trajectories with variable ballistic coefficients.[15] Warden utilized the Allen-Eggers solution, but allowed β to vary with altitude such that:

$$\beta = \beta_0 \left[1 - C\left(1 - \bar{h}\right)\right]^n \tag{2}$$

This formulation enables one to model either monotonically increasing or decreasing ballistic coefficient as a function of the normalized altitude, $\bar{h}$, dependent on the value of n. Warden was able to derive expressions for velocity and acceleration as functions of altitude, as well as a truncated series approximation for peak acceleration and a transcendental expression for the altitude at peak acceleration. The presence of special functions, such as the complete and incomplete Γ functions, make Warden's solution relatively complicated.

Modeling a variable ballistic coefficient has also been studied as a method for improving the accuracy of analytical trajectory solutions. In 1965, M. Cohen developed expressions for velocity and flight-path angle as functions of altitude by utilizing a specific drag program,[16] where the drag coefficient was modeled as:

$$C_D = C\rho \sin\gamma \tag{3}$$

More recently, Barbera modeled the variation in drag coefficient as a piecewise function of:

$$C_D = C_i V^{n_i} \tag{4}$$

This model was based on empirical aerodynamics data. Barbera used the model to better capture the hypersonic and supersonic variations in drag coefficient for blunted cones.[17] While Barbera's results indicated good accuracy, the study was limited to small cone half angles (less than 8 deg) and large ballistic coefficients (near 10,000 kg/m^2). These properties are typical of strategic reentry systems. In comparison, the sphere-cone capsules flown at Mars have half angles of 70 deg.

The Allen-Eggers Solution

The solution of Allen and Eggers may be arrived at by neglecting gravity and lift and assuming a constant flight-path angle in the two-degree-of-freedom equations of motion for planetary entry. This results in a relatively simple relationship between atmospheric density and velocity:[18]

$$V_2 = V_1 \exp\left[\frac{H\left(\rho_2 - \rho_1\right)}{2\beta \sin\gamma^*}\right] \tag{5}$$

where γ^* is the assumed constant flight-path angle. Using this relationship, closed-form expressions for sensed acceleration and stagnation-point heat rate may be derived, as well as expressions for trajectory states at peak values of these quantities.

The expression for sensed acceleration, in terms of the density, is:

$$a_2 = \frac{\rho_2}{2\beta g} V_1^2 \exp\left[\frac{H\left(\rho_2 - \rho_1\right)}{\beta \sin\gamma^*}\right] \tag{6}$$

The conditions at peak sensed acceleration are then, with respect to the initial velocity:

$$V_{a_{max}} = \frac{V_0}{\sqrt{e}} \tag{7}$$

$$a_{max} = -\frac{\sin\gamma^*}{2egH} V_0^2 \tag{8}$$

The expression for the stagnation-point convective heat rate is:

$$\dot{Q}_2 = k\sqrt{\frac{\rho}{r}} V_0^3 \exp\left[\frac{3H\left(\rho_2 - \rho_1\right)}{2\beta \sin\gamma^*}\right] \tag{9}$$

And the peak heat rate is given by:

$$\dot{Q}_{max} = k\sqrt{-\frac{\beta \sin\gamma^*}{3eHr}} V_0^3 \tag{10}$$

Eq. (5) through (10) make no assumptions about the density profile of the atmosphere.

The range is given by:

$$s_2 = R\cot\gamma^* \left(\ln\left\{H\ln\left[\frac{\rho_1}{\rho_{ref}} + \frac{\beta\sin\gamma^*}{H\rho_{ref}}\ln\left(\frac{V_2^2}{V_1^2}\right)\right] - R\right\} - \ln\left\{H\ln\left[\frac{\rho_1}{\rho_{ref}}\right] - R\right\}\right) \tag{11}$$

The constant flight-path angle may be computed using relationships developed by Citron and Meir[19] applied at peak acceleration,[20] so that γ^* may be determined as a function of the initial conditions:

$$\sin\gamma^* = \sin\gamma_0\left(2F^* - 1\right) \tag{12}$$

where

$$F^* = \left[1 + \frac{H}{R\tan^2\gamma_0}\left\{C_F\frac{V_C^2}{V_0^2} + \left(\frac{V_C^2}{V_0^2} - 1\right)\ln\left(1 - \frac{\beta\sin\gamma_0}{H\rho_0}\right)\right\}\right]^{1/2} \tag{13}$$

and

$$C_F = \mathrm{Ei}(1) - \bar{\gamma} \approx 1.3179 \tag{14}$$

ANALYTICAL STUDY OF DISCRETE-EVENT SYSTEMS

The enhanced Allen-Eggers solution may be used to assess drag-modulation trajectory-control systems for planetary entry.[20] Consider an entry vehicle capable of discrete-event drag-modulation trajectory control that modulates its drag by reducing drag area through a single jettison event at a particular point during entry. The drag-area jettison is assumed to be instantaneous; vehicle properties are constant on either side of the jettison. These properties may be described by the pre-jettison

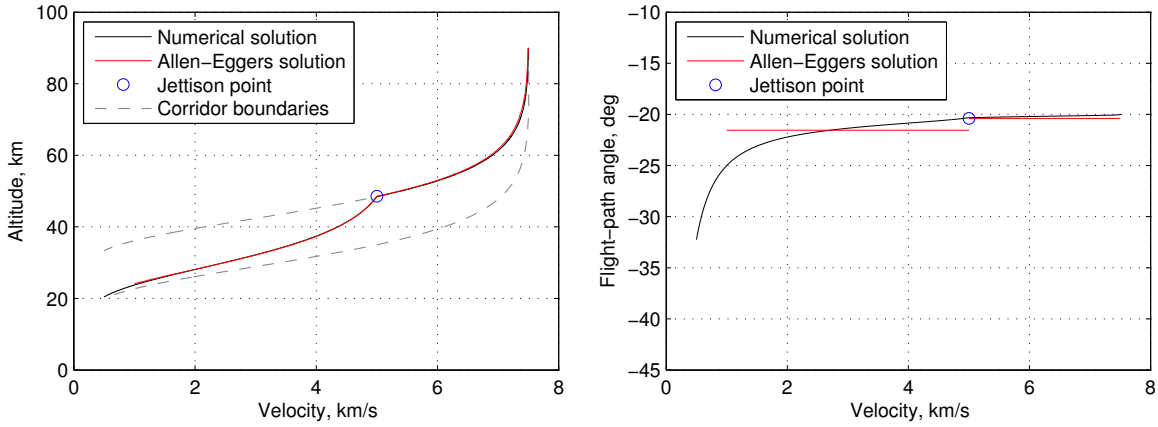

(a) Altitude

(b) Flight-path angle

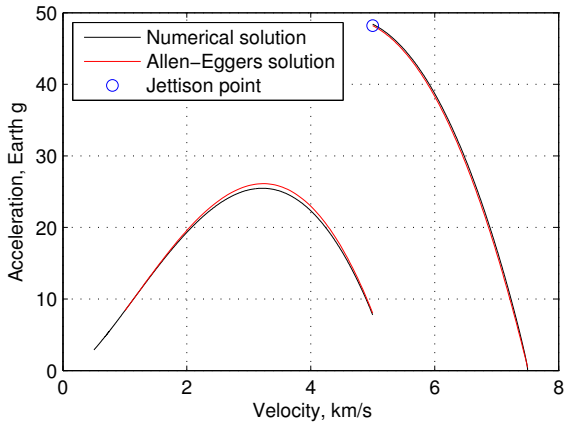

(c) Acceleration

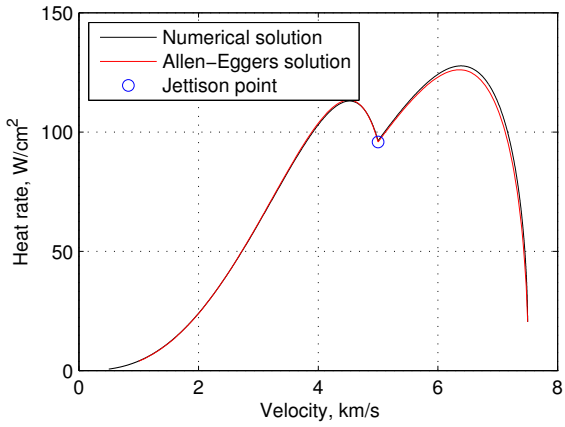

(d) Heat rate

Figure 2. Example application of the Allen-Eggers solution.

ballistic coefficient, β_0, and post-jettison ballistic coefficient, β_1. Furthermore, we will assume that $\beta_1 > \beta_0$.

An example application is shown in Fig. 2. For this trajectory (parameters given in Table 1), agreement between numerical integration of the equations of motion and the Allen-Eggers solution is excellent. The trajectory is constructed using two separate, constant ballistic coefficient segments that join at the jettison point. The first segment starts from the initial condition in Table 1 with $\beta = \beta_0$. The second segment has $\beta = \beta_1$; the jettison point serves as the initial condition for the second trajectory segment, where $V_{0,1} = V_1$, $h_{0,1} = f(V_1)$, and $\gamma_{0,2} = \gamma_0^*$.

The altitude-velocity plot (Fig. 2(a)) shows the corridor-bounding trajectories for this initial state. These trajectories correspond to the cases where no jettison occurs (entry with constant $\beta = \beta_0$) and where jettison occurs at the initial state (entry with constant $\beta = \beta_1$). Figure 2(c) shows the discrete change in acceleration at jettison; Figure 2(d) shows the discrete change in the rate of change of the heat rate.

Table 1. Nominal Parameters for Example Trajectory

Parameter	Value
Planet	Earth
V_0	7500 m/s
γ_0	-20 deg
h_0	90 km
β_0	50 kg/m^2
β_1	300 kg/m^2
V_1	5000 m/s

Range Control Authority

The Allen-Eggers solution may be used to show analytically how changes in ballistic coefficient may be used to control range during entry. By varying the jettison velocity, a drag-modulation entry vehicle may control its range (see Fig. 3). The maximum possible range occurs when jettison occurs immediately, resulting in constant-β flight at maximum β, β_1. The minimum possible range occurs when no jettison occurs, resulting in constant-β flight at the minimum β, β_0.

The control authority metric for drag-modulation trajectory control systems is ratio of the maximum to minimum ballistic coefficients, or β_1/β_0. This may be shown analytically, starting with the Allen-Eggers equation for range-to-go over a flat planet:

$$s_{togo} = \cot\gamma^* \left(h_f - h\right) \tag{15}$$

The divert capability at jettison for a discrete-event drag-modulation system is:

$$\Delta s = \overbrace{\cot\gamma_1^* \left(h_f - h_J\right)}^{\text{max. range}} - \overbrace{\cot\gamma_0^* \left(h_f - h_J\right)}^{\text{min. range}} \tag{16}$$

Altitude may be written as a function of velocity and ballistic coefficient through the Allen-Eggers altitude-velocity profile:

$$h = h_{ref} - H \ln\left[\frac{\beta \sin\gamma^*}{\rho_{ref} H} \ln\left(\frac{V^2}{V_1^2}\right) + \frac{\rho_1}{\rho_{ref}}\right] \tag{17}$$

If we choose our reference point (denoted by subscript 1 above) to be the jettison velocity, we find:

$$\begin{aligned}\Delta s = \cot\gamma_1^* \left(H \ln\left[\frac{\beta_1 \sin\gamma_1^*}{\rho_{ref} H} \ln\left(\frac{V_f^2}{V_1^2}\right) + \frac{\rho_1}{\rho_{ref}}\right] - H \ln\left[\frac{\rho_1}{\rho_{ref}}\right]\right) \\ - \cot\gamma_0^* \left(H \ln\left[\frac{\beta_0 \sin\gamma_0^*}{\rho_{ref} H} \ln\left(\frac{V_f^2}{V_1^2}\right) + \frac{\rho_1}{\rho_{ref}}\right] - H \ln\left[\frac{\rho_1}{\rho_{ref}}\right]\right)\end{aligned} \tag{18}$$

Assuming that $\gamma_0^* \approx \gamma_1^*$ for the same γ_0, this equation simplifies to:

$$\Delta s = H \cot\gamma^* \ln\left[\frac{\frac{\beta_1 \sin\gamma^*}{\rho_{ref} H} \ln\left(\frac{V_f^2}{V_1^2}\right) + \frac{\rho_1}{\rho_{ref}}}{\frac{\beta_0 \sin\gamma^*}{\rho_{ref} H} \ln\left(\frac{V_f^2}{V_1^2}\right) + \frac{\rho_1}{\rho_{ref}}}\right] \tag{19}$$

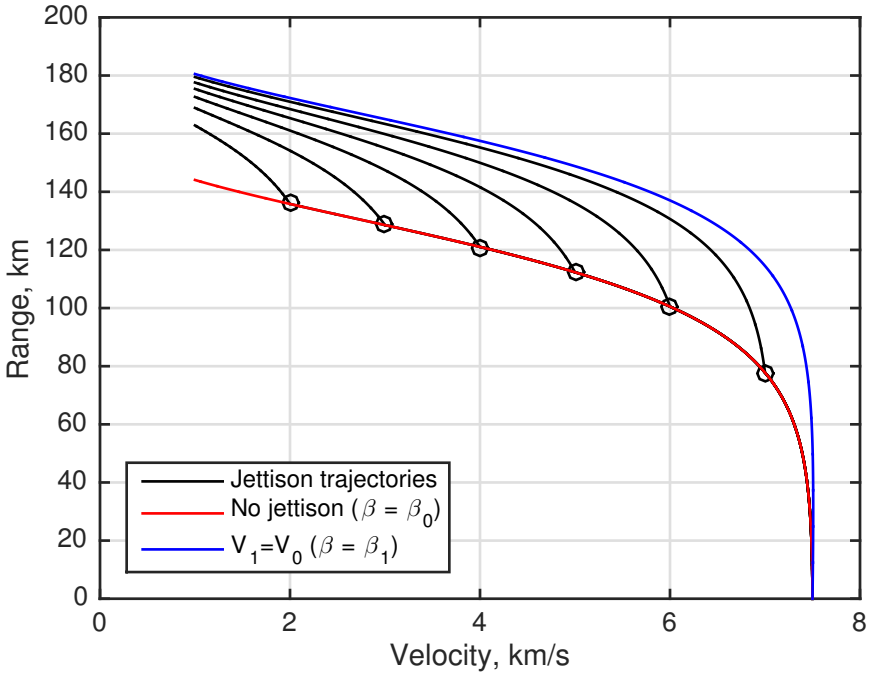

Figure 3. Range profiles for several jettison velocities.

Further, recognizing that ρ_1 is given by:

$$\rho_1 = \frac{\beta_0 \sin\gamma_0^*}{H} \ln\left(\frac{V_1^2}{V_0^2}\right) + \rho_0 \tag{20}$$

and neglecting ρ_0 relative to ρ_{ref}, we find:

$$\Delta s = H \cot\gamma^* \ln\left[\frac{(\beta_1/\beta_0)\ln\left(V_f^2/V_1^2\right) + \ln\left(V_1^2/V_0^2\right)}{\ln\left(V_f^2/V_0^2\right)}\right] \tag{21}$$

This shows the divert capability is a function of the initial and final velocities, the jettison velocity, the ballistic coefficient ratio, and the flight-path angle. The dependence on trajectory parameters is intuitive, but the sole dependence on ballistic coefficient ratio (as opposed to the magnitude of the ballistic coefficients) is not.

The maximum divert capability occurs at the top of the atmosphere. For maximum range, jettison occurs at a high altitude relative to h_{ref}, making the ρ_1/ρ_{ref} term small enough to be neglected in Eq. (19). This results in:

$$\Delta s_{max} = -H \cot\gamma^* \ln\left(\frac{\beta_1}{\beta_0}\right) \tag{22}$$

This equation shows the relationship between Δs_{max} and β ratio. Increasing the ratio results in a larger maximum divert capability and increased range control authority. The maximum divert range is a weaker function of the magnitude of the ballistic coefficients, which influences the value of γ^*.

Figure 4 shows the maximum divert capability, i.e. Δs at V_0, across a range of values for (β_0, β_1). Numerical integration of the equations of motion is shown in Fig. 4(a); computation using Allen-Eggers is shown in Fig. 4(b). Lines of constant ballistic coefficient ratio are shown in white. The

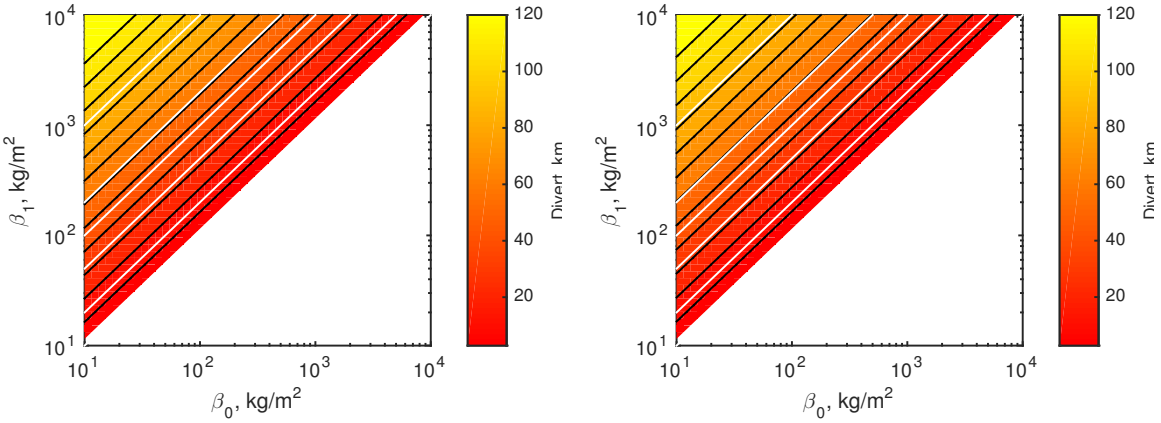

(a) Numerical integration (b) Allen-Eggers

Figure 4. Divert capability over a range of ballistic coefficients.

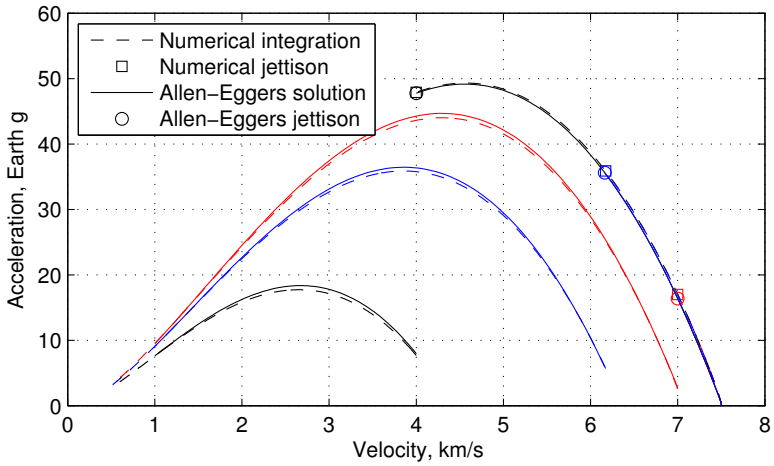

Figure 5. Acceleration profiles for several jettison velocities.

results nearly identical, showing that the Allen-Eggers solution is accurate. Also, it is clear that divert capability is primarily a function of ballistic coefficient ratio: divert capability increases with increasing β ratio. In this manner, the ballistic coefficient ratio is analogous to the lift-to-drag ratio (L/D) for lift-modulation systems.

Minimizing Peak Sensed Acceleration

Figure 5 shows the effect of different jettison velocities on the peak acceleration. If the jettison occurs after the β_0 peak acceleration, then the β_1 acceleration pulse is much smaller and does not affect the peak value (black curves). If the jettison occurs early in the trajectory, the opposite occurs: the acceleration pulse for the β_1 trajectory segment is relatively large and dictates the peak acceleration (red curve). From the figure, one can see that an intermediate velocity will occur when the acceleration at jettison is equal to the peak acceleration in the β_1 trajectory segment. The Allen-Eggers solution may be used to derive an analytical solution for this jettison point.

The acceleration at jettison is:

$$a_{1,J} = \frac{\rho_1}{2\beta g} V_1^2 = \frac{V_1^2}{2\beta_0 g} \left(\frac{\beta_0 \sin\gamma_0^*}{H} \ln\left(\frac{V_1^2}{V_0^2}\right) + \rho_0 \right) \tag{23}$$

The peak acceleration for the β_1 trajectory segment is given by:

$$a_{2,max} = -\frac{\sin\gamma_1^*}{2egH} V_1^2 \exp\left(-\frac{H\rho_1}{\beta_1 \sin\gamma_1^*}\right) \tag{24}$$

Setting Eq. (23) and (24) equal and eliminating common factors, we find:

$$-\frac{\sin\gamma_1^*}{eH} \exp\left(-\frac{H\rho_1}{\beta_1 \sin\gamma_1^*}\right) = \frac{\rho_1}{\beta_0} \tag{25}$$

The density at jettison is given by Eq. (20). If we assume ρ_0 is small relative to the other term in Eq. (20) and substitute for ρ_1 in Eq. (25), we find:

$$-\frac{\sin\gamma_1^*}{e} \exp\left(-\frac{\beta_0 \sin\gamma_0^* \ln\left(V_1^2/V_0^2\right)}{\beta_1 \sin\gamma_1^*}\right) = \sin\gamma_0^* \ln\left(\frac{V_1^2}{V_0^2}\right) \tag{26}$$

Taking the natural logarithm of both sides and rearranging yields:

$$-\frac{\beta_0}{\beta_1}\frac{\sin\gamma_0^*}{\sin\gamma_1^*} \ln\left(\frac{V_1^2}{V_0^2}\right) = \ln\left[\frac{\sin\gamma_0^*}{\sin\gamma_1^*} \ln\left(\frac{V_1^2}{V_0^2}\right)\right] + 1 \tag{27}$$

If we further assume that $\sin\gamma_0^* / \sin\gamma_1^* \approx 1$ and rearrange in terms of the ballistic coefficient ratio, we find:

$$\frac{\beta_1}{\beta_0} = \frac{\ln\left(V_0^2/V_1^2\right)}{\ln\left[\ln\left(V_0^2/V_1^2\right)\right] + 1} \tag{28}$$

This relationship gives the jettison velocity for minimum peak acceleration for a particular β ratio. Beyond the Allen-Eggers assumptions, this relationship only assumes that the initial density at the top of the atmosphere is negligible and that the corrected constant flight path angles are of similar magnitudes. While this relationship is unfortunately transcendental in V_1, it does show that the jettison velocity for minimum a_{max} (as a fraction of V_0) is only a function of the ballistic coefficient ratio, not the magnitude of the ballistic coefficients, planetary parameters, or the initial flight-path angle.

To test the validity of this equation, it may be compared to two other solution methods: 1. numerical minimization coupled with numerical integration of the equations of motion and 2. direct solution of Eq. (25) via numerical root-finding. Figure 6 shows the jettison velocity associated with minimum a_{max} over a range of different ballistic-coefficient pairs evaluated using the two different methods. Lines of constant ballistic-coefficient ratio are shown in white. The lower right half of the figure represents β ratios less than one, or $\beta_0 > \beta_1$. This case is not considered, since it violates the assumed acceleration profile. Also, the jettison velocity is not defined for a β ratio of one, since $\beta_0 = \beta_1$. The figure shows that jettison velocity for minimum a_{max} appears to be a function of ballistic coefficient only. The velocity decreases with decreasing β ratio, but is relatively constant for a large range of β ratios (those above about 5). Agreement between the a) numerical solution and b) Allen-Eggers solution appears to be good in both trend and overall magnitude.

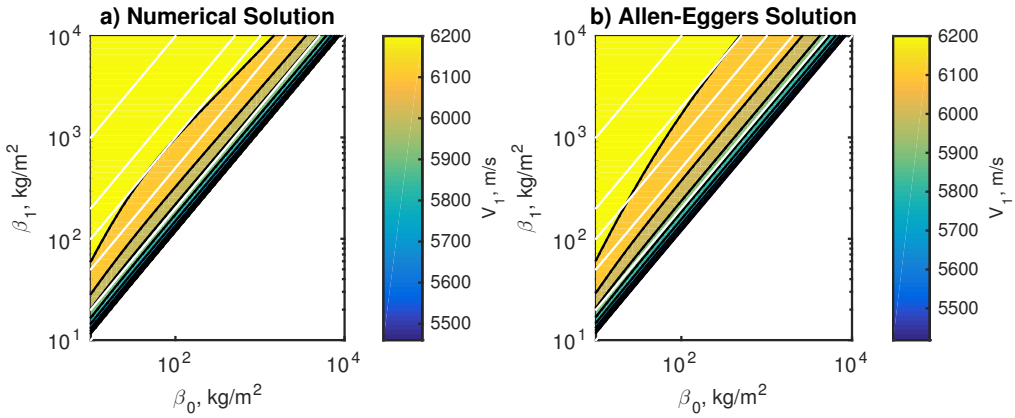

Figure 6. Jettison velocity for minimum a_{max} as a function of (β_0, β_1).

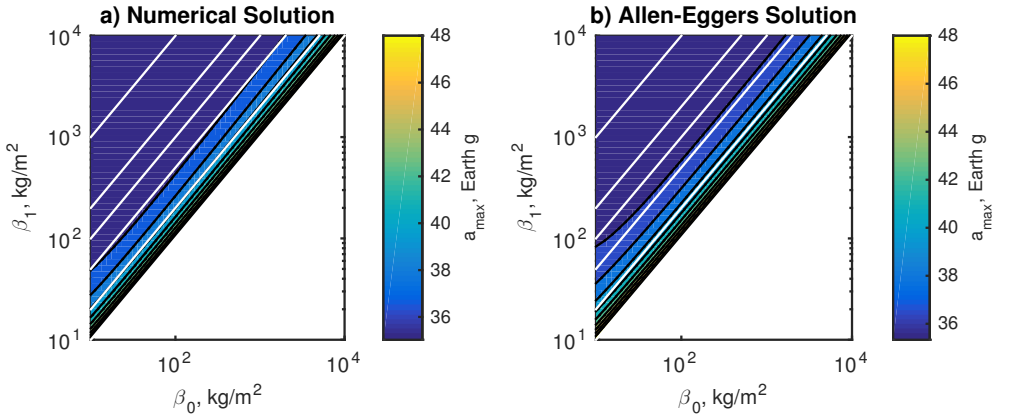

Figure 7. Minimum a_{max} as a function of (β_0, β_1).

Figure 7 shows the minimum a_{max} associated with the jettison velocities in Figure 6. Again, agreement is good between the two methods and a similar trend is seen where a_{max} is only a function of ballistic-coefficient ratio. The peak acceleration increases with decreasing ballistic coefficient ratio, but is relatively flat for ballistic coefficient ratios above about 5. The maximum peak acceleration shown is 48 g, which corresponds to the case where $\beta_0 = \beta_1$. This is the acceleration for this particular trajectory for a vehicle with a constant ballistic coefficient. The lower values of a_{max} shown in the figure show the ability of a drag-modulation system to reduce peak acceleration.

To compare the two methods shown in Figures 6 and 7, as well as the relationship proposed in Eq. (28), the data points for these figures are plotted as a function of ballistic coefficient ratio in Figure 8 and Figure 9. Figure 8 shows that there is excellent agreement between the numerical solution and the Allen-Eggers solution. It also shows that Eq. (28) effectively predicts the trend in jettison velocity. The agreement in Figure 9 is also good: the Allen-Eggers prediction of the peak acceleration is within 3% of the numerical solution.

The reduction in peak acceleration can be quantified as the drag-modulation a_{max} over the a_{max}

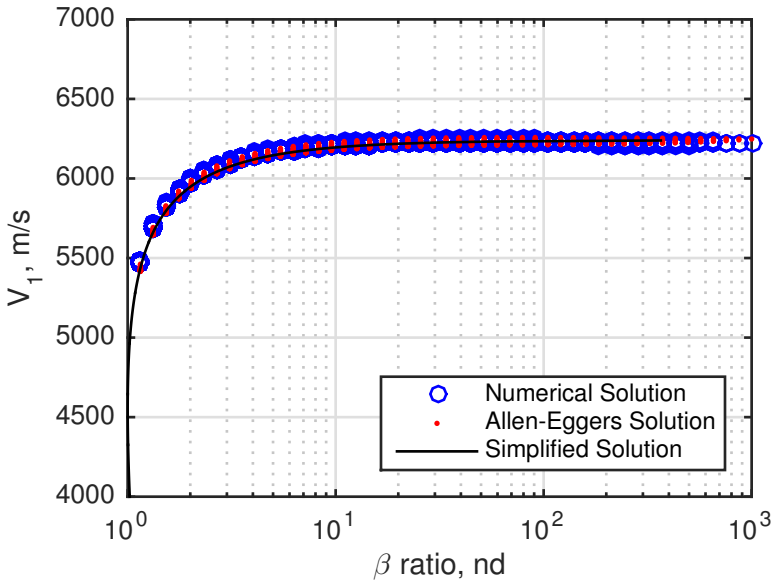

Figure 8. Jettison velocity for minimum a_{max} as a function of ballistic coefficient ratio.

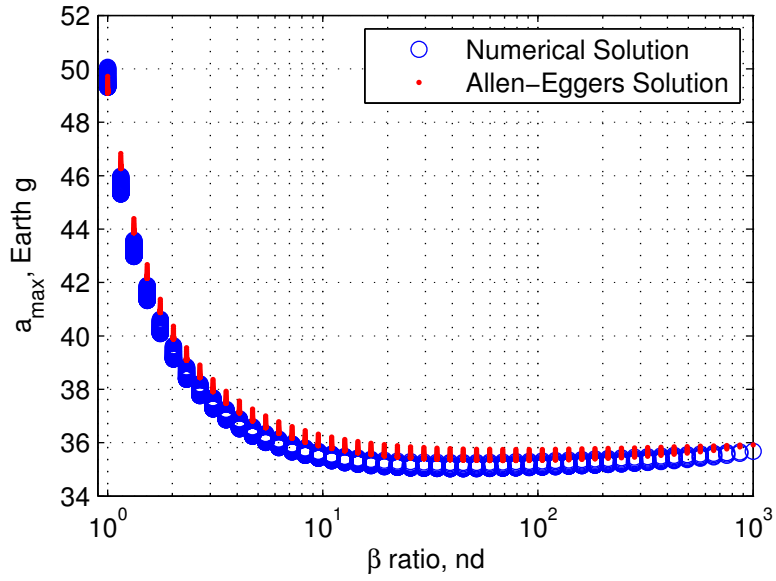

Figure 9. Minimum a_{max} as a function of ballistic coefficient ratio.

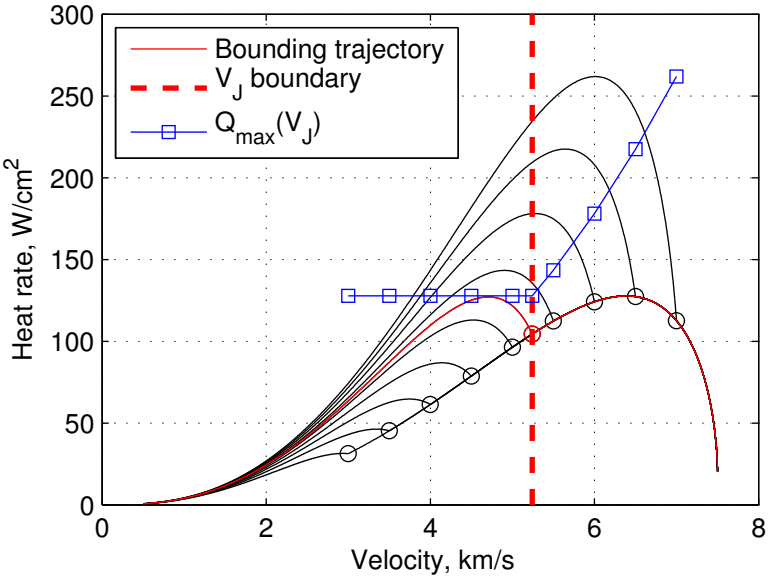

Figure 10. Heat rate as a function of velocity for several jettison velocities.

associated with a constant-β_0 trajectory. It turns out to be (again, neglecting ρ_0 relative to ρ_1):

$$\frac{a_{DM}}{a_{max}} = e\frac{V_1^2}{V_0^2}\ln\left(\frac{V_0^2}{V_1^2}\right) \tag{29}$$

This expression shows that the reduction in peak acceleration is only a function of jettison velocity as a fraction of the initial velocity, which in turn is only a function of ballistic-coefficient ratio (see Eq. (28)).

Minimizing Peak Stagnation-Point Heat Rate

Larger ballistic coefficients imply flight at lower altitude (and correspondingly higher density) and smaller effective nose radii, increasing in heat rate. With this in mind, it becomes apparent that the best way to minimize peak heat rate during entry is to maintain a low ballistic coefficient through peak heating. After the initial heat pulse, changing to a higher ballistic coefficient may still cause the heat rate to rise above the previous peak if the jettison velocity is too close to the velocity at the first peak (see Fig. 10). An expression may be derived for a limit on the jettison velocity such that the peak of the initial heat-rate pulse is not exceeded.

To determine the jettison velocities that minimize peak heat rate, we start by enforcing the condition:

$$\dot{Q}_{max,1} > \dot{Q}_{max,2} \tag{30}$$

We can use the Allen-Eggers solution to write expressions for these peak heat rates in terms of known trajectory parameters:

$$k\sqrt{-\frac{\beta_0\sin\gamma_0^*}{3eHr_{n,1}}}V_0^3\exp\left(-\frac{3H\rho_0}{2\beta_0\sin\gamma_0^*}\right) > k\sqrt{-\frac{\beta_1\sin\gamma_1^*}{3eHr_{n,2}}}V_1^3\exp\left(-\frac{3H\rho_1}{2\beta_1\sin\gamma_1^*}\right) \tag{31}$$

Substituting Eq. (20) for ρ_1 and neglecting ρ_0 because it is small relative to other densities, we find:

$$k\sqrt{-\frac{\beta_0 \sin\gamma_0^*}{3eHr_{n,1}}}V_0^3 > k\sqrt{-\frac{\beta_1 \sin\gamma_1^*}{3eHr_{n,2}}}V_1^3 \exp\left(-\frac{3H}{2\beta_1 \sin\gamma_1^*}\frac{\beta_0 \sin\gamma_0^*}{H}\ln\frac{V_1^2}{V_0^2}\right) \tag{32}$$

Simplifying leads to:

$$\sqrt{\frac{\beta_0}{\beta_1}\frac{\sin\gamma_0^*}{\sin\gamma_1^*}\frac{r_{n,2}}{r_{n,1}}}V_0^3 > V_1^3 \exp\left(-\frac{3}{2}\frac{\beta_0 \sin\gamma_0^*}{\beta_1 \sin\gamma_1^*}\ln\frac{V_1^2}{V_0^2}\right) \tag{33}$$

Taking the natural logarithm to map the multiplication above to addition yields:

$$\frac{1}{2}\ln\left(\frac{\beta_0}{\beta_1}\frac{\sin\gamma_0^*}{\sin\gamma_1^*}\frac{r_{n,2}}{r_{n,1}}\right) + 3\ln V_0 > 3\ln V_1 - 3\frac{\beta_0}{\beta_1}\frac{\sin\gamma_0^*}{\sin\gamma_1^*}(\ln V_1 - \ln V_0) \tag{34}$$

Grouping like terms and solving for V_1 leads to a condition on V_1 for minimizing the peak heat rate:

$$V_1 < V_0 \exp\left[\frac{\ln\left(\frac{\beta_0}{\beta_1}\frac{\sin\gamma_0^*}{\sin\gamma_1^*}\frac{r_{n,2}}{r_{n,1}}\right)}{6\left(1-\frac{\beta_0}{\beta_1}\frac{\sin\gamma_0^*}{\sin\gamma_1^*}\right)}\right] \tag{35}$$

If one assumes that $\sin\gamma_0^* \approx \sin\gamma_1^*$ and that the effective nose radius does not change across the jettison event, this inequality reduces to:

$$V_1 < V_0 \exp\left[\frac{(\beta_1/\beta_0)\ln(\beta_1/\beta_0)}{6(1-\beta_1/\beta_0)}\right] \tag{36}$$

Figure 10 shows the effect of varying jettison time on the heat rate (trajectory parameters are given in Table 1), the proposed jettison velocity limit in Eq. (36), and the peak heat rate as a function of jettison velocity for the example trajectory (see Table 1). The proposed limit on the jettison velocity to limit the peak heat rate appears to be correct–at this jettison velocity, the two peaks of the heat pulse are nearly equal. The trajectory data in this figure were generated using numerical integration, but it agrees well with the proposed analytical condition on jettison velocity.

Multi-Stage Systems

Eq. (20) may be used to relate the density and velocity at the nth jettison point in an N-stage system:

$$\rho_{n+1} = \rho_0 + \sum_{i=0}^{n}\frac{\beta_i \sin\gamma_i^*}{H}\ln\left(\frac{V_{i+1}^2}{V_i^2}\right) \tag{37a}$$

$$V_{n+1} = V_0\left\{\prod_{i=0}^{n}\exp\left[\frac{H(\rho_{i+1}-\rho_i)}{2\beta_i \sin\gamma_i^*}\right]\right\} \tag{37b}$$

where

$$\sin\gamma_{n+1}^* = \sin\gamma_n^*(2F_n^* - 1) \tag{38}$$

and

$$F_n^* = \left[1 + \frac{H}{R\tan^2\gamma_n^*}\left\{C\frac{V_C^2}{V_n^2} + \left(\frac{V_C^2}{V_n^2} - 1\right)\ln\left(1 - \frac{\beta_n \sin\gamma_n^*}{H\rho_n}\right)\right\}\right]^{1/2} \tag{38a}$$

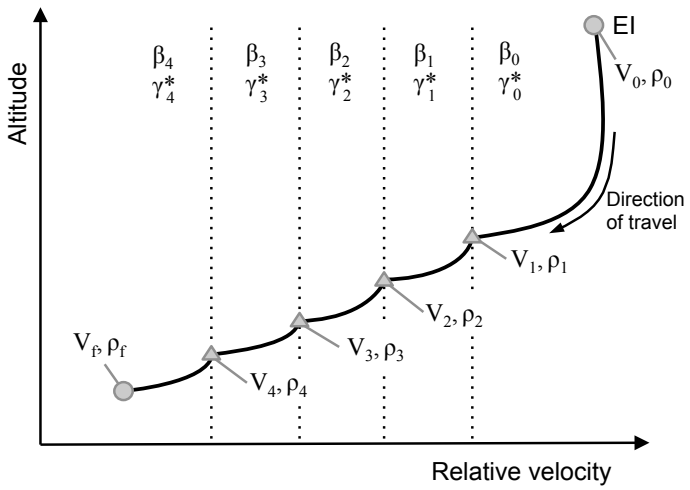

Figure 11. Example of a discrete drag-modulation system with 5 stages and 4 jettison events.

Minimizing peak acceleration. Using a method similar to the above, a trajectory that minimizes peak acceleration for an N-stage system may be computed analytically. First, one must solve this transcendental equation for the density at the final jettison point, ρ_{N-1}:

$$\rho_{N-1} = \frac{-\beta_{N-2} \sin \gamma_{N-1}^*}{H} \exp\left(\frac{-H\rho_{N-1}}{\beta_{N-1} \sin \gamma_{N-1}^*} - 1\right) \tag{39}$$

This result may be used to solve for ρ_n for the remaining stages:

$$\frac{\rho_{n+1}}{\rho_n} = \frac{\beta_n}{\beta_{n-1}} \exp\left[\frac{H\rho_n(1 - \rho_{n+1}/\rho_n)}{\beta_n \sin \gamma_n^*}\right] \tag{40}$$

Jettison velocities may then be computed using Eq. (37b).

From Eq. (40), one can see that the ratio of the densities at jettison is always less than that of the ballistic coefficients, i.e.:

$$\rho_{n+1}/\rho_n < \beta_n/\beta_{n-1} \tag{41}$$

This relationship establishes a bound on where the jettison should occur. From a practical standpoint, solving Eq. (39) and (40) may be numerically difficult because, in general, γ_n^* is a function of γ_{n-1}^*, ρ_{n-1}, and V_{n-1}.

Limiting peak heat rate. To minimize peak heat rate, we require that the peak heat rate of any particular segment in a multi-stage trajectory be less than the previous stage:

$$\dot{Q}_{max,n+1} < \dot{Q}_{max,n} \tag{42}$$

Applying the Allen-Eggers solution and simplifying yields::

$$\ln\left[\left(\frac{r_n}{r_{n+1}}\right)\left(\frac{\beta_{n+1} \sin \gamma_{n+1}^*}{\beta_n \sin \gamma_n^*}\right)\right] + 6 \ln\left(\frac{V_{n+1}}{V_n}\right) + 3H\left(\frac{\rho_n}{\beta_n \sin \gamma_n^*} - \frac{\rho_{n+1}}{\beta_{n+1} \sin \gamma_{n+1}^*}\right) < 0 \tag{43}$$

Eliminating the velocities using Eq. (20) results in:

$$\ln\left[\left(\frac{r_n}{r_{n+1}}\right)\left(\frac{\beta_{n+1} \sin \gamma_{n+1}^*}{\beta_n \sin \gamma_n^*}\right)\right] + 3H\rho_{n+1}\left(\frac{1}{\beta_n \sin \gamma_n^*} - \frac{1}{\beta_{n+1} \sin \gamma_{n+1}^*}\right) < 0 \tag{44}$$

If one neglects the differences between the flight-path angles and nose radii, one finds that:

$$\rho_{n+1} < \frac{\beta_n \sin\gamma^* \ln\left(\beta_n/\beta_{n+1}\right)}{3H\left(1-\beta_n/\beta_{n+1}\right)} \tag{45}$$

where γ^* is an average value over n and $n+1$. This relationship provides a bound on the density (and therefore altitude) of the next jettison event to maintain the minimum peak heat rate throughout the entry trajectory.

CONCLUSION

The enhanced Allen-Eggers solution for ballistic entry was applied to discrete-event drag- modulation systems and was shown to accurately reproduce trajectories relative to numerical solutions to the planar equations of motion. Closed-form analytical relationships were developed that show ballistic coefficient ratio is the control authority metric for drag-modulation systems: ballistic coefficient ratio governs range control authority, peak acceleration reduction capability, and the jettison velocity associated with minimum peak heat rate. The closed-form relationships are appropriate for applications in which execution speed and simplicity are paramount, such as onboard real-time guidance and targeting.

ACKNOWLEDGMENT

This work was supported in part by a NASA Space Technology Research Fellowship.

NOTATION

a	sensed acceleration magnitude, Earth g
C	constant
C_D	hypersonic drag coefficient
e	base of the natural logarithm
g	acceleration due to gravity, m/s^2
h	altitude, m
H	atmospheric scale height, m
i	integer index
k	stagnation-point heating constant kg$^{1/2}$/m
m	mass, kg
n	integer
N	integer
$\dot{Q}$	stagnation-point heat rate, W/cm^2
r	effective nose radius, m
R	planetary radius, m
s	range, km
S_{ref}	aerodynamic reference area, m^2
V	velocity magnitude, m/s
V_i	velocity magnitude at jettison, m/s
β	ballistic coefficient, kg/m^2
γ	flight-path angle, rad
$\bar{\gamma}$	Euler-Mascheroni constant
ρ	atmospheric density, kg/m^3
ρ_i	atmospheric density at jettison, kg/m^3

REFERENCES

[1] L. L. Levy, "The Use of Drag Modulation to Limit the Rate at Which Deceleration Increases During Nonlifting Entry," Tech. Rep. NASA TN D-1037, Ames Research Center, Washington, DC, Sept. 1961.

[2] P. H. Rose and J. E. Hayes, "Drag Modulation and Celestial Mechanics," *7th Annual Meeting of the American Astronautical Society*, Dallas, TX, Jan. 1961.

[3] Z.-S. Kuo, K.-C. Liu, and Y.-S. Chang, "Explicit Guidance of Ballistic Entry Using Improved Matched Asymptotic Expansions," *Transactions of the Japan Society for Aeronautical and Space Sciences*, Vol. 50, Jan. 2007, pp. 121–127.

[4] A. D. McRonald, "A Lightweight Inflatable Hypersonic Drag Device for Planetary Entry," *Association Aeronautique de France Conference*, Arcachon, France, Mar. 1999.

[5] C. H. Westhelle and J. P. Masciarelli, "Assessment of Aerocapture Flight at Titan Using a Drag-only Device," *AIAA Atmospheric Flight Mechanics Conference and Exhibit*, Austin, TX, Aug. 2003, pp. 1–7.

[6] J. L. Hall and A. K. Le, "Aerocapture Trajectories for Spacecraft with Large Towed Ballutes," *AAS/AIAA Space Flight Mechanics Meeting*, Santa Barbara, CA, Feb. 2001.

[7] N. X. Vinh, J. R. Johannesen, K. D. Mease, and J. M. Hanson, "Explicit guidance of drag-modulated aeroassisted transfer between elliptical orbits," *Journal of Guidance, Control, and Dynamics*, Vol. 9, May 1986, pp. 274–280.

[8] K. L. Miller, D. Gulick, J. Lewis, B. Trochman, J. Stein, D. T. Lyons, and R. G. Wilmoth, "Trailing Ballute Aerocapture: Concept and Feasibility Assessment," *39th AIAA/ASME/SAE/ASEE Joint Propulsion Conference and Exhibit*, Huntsville, AL, July 2003.

[9] W. R. Johnson and D. T. Lyons, "Titan Ballute Aerocapture Using a Perturbed TitanGRAM Model," *AIAA Atmospheric Flight Mechanics Conference and Exhibit*, Providence, RI, Aug. 2004.

[10] Z. R. Putnam and R. D. Braun, "Drag-Modulation Flight-Control System Options for Planetary Aerocapture," *Journal of Spacecraft and Rockets*, Aug. 2013, pp. 1–12.

[11] Z. R. Putnam and R. D. Braun, "Precision Landing at Mars Using Discrete-Event Drag Modulation," *Journal of Spacecraft and Rockets*, Vol. 51, Feb. 2014, pp. 128–138.

[12] R. L. Phillips and C. B. Cohen, "Use of Drag Modulation to Reduce Deceleration Loads During Atmospheric Entry," *ARS Journal*, Vol. 29, June 1959, pp. 414–422.

[13] A. Robinson and A. Besonie, "On the Problems of Re-Entry into the Earth's Atmosphere," *Journal of the Astronautical Sciences*, Vol. 7, Apr. 1960, pp. 7–21.

[14] D. E. Randall, "Influence of staging on re-entry trajectory characteristics," *Journal of Spacecraft and Rockets*, Vol. 7, Mar. 1970, pp. 370–372.

[15] R. V. Warden, "Ballistic Re-Entries With a Varying W/CD A," *ARS Journal*, Vol. 31, Feb. 1961, pp. 208–213.

[16] M. J. Cohen, "Some Closed Form Solutions to the Problem of Re-Entry of Lifting and Non-Lifting Vehicles," *2nd Aerospace Sciences Meeting*, New York, NY, Northhampton College of Advanced Technology, American Institute of Aeronautics and Astronautics, Jan. 1965.

[17] F. J. Barbera, "Closed-Form Solution for Ballistic Vehicle Motion," *Journal of Spacecraft and Rockets*, Vol. 18, Jan. 1981, pp. 52–57.

[18] H. J. Allen and A. J. Eggers, "A Study of the Motion and Aerodynamic Heating of Ballistic Missiles Entering the Earth's Atmosphere at High Supersonic Speeds," Tech. Rep. NACA-TR-1381, Ames Aeronautical Laboratory, Washington, DC, 1958.

[19] S. J. Citron and T. C. Meir, "An analytic solution for entry into planetary atmospheres," *AIAA Journal*, Vol. 3, Mar. 1965, pp. 470–475.

[20] Z. R. Putnam and R. D. Braun, "Extension and Enhancement of the Allen-Eggers Solution for Ballistic Entry Trajectories," *Journal of Guidance, Control, and Dynamics*, Jan. 2015.